

# Frequency-doubling of a CW fiber laser using PPKTP, PPMgSLT, and PPMgLN

F. J. Kontur, I. Dajani, Yalin Lu, and R. J. Knize

Laser and Optics Research Center, Physics Department, 2354 Fairchild Dr, Ste 2A31, USAF Academy, CO 80840  
[frederick.kontur.ctr@usafa.af.mil](mailto:frederick.kontur.ctr@usafa.af.mil)

**Abstract:** Second-harmonic generation (SHG) in PPKTP, PPMgSLT, and PPMgLN crystals is analyzed by frequency-doubling CW light from a 1064 nm fiber laser over a range of powers up to 10 W. Data for fundamental powers less than 3 W is used to determine the effects of the fundamental laser linewidth on SHG and to identify imperfections in the periodicity and boundary sharpness of the crystals' poled domains which can reduce SHG. Data for fundamental powers greater than 3 W is used to diagnose and model limiting effects on SHG such as pump depletion and thermal dephasing. Thermal dephasing was found to reduce second-harmonic power by 25% or more for input fundamental powers approaching 10 W.

©2007 Optical Society of America

OCIS codes: (190.2620) Frequency conversion; (190.4400) Nonlinear optics, materials.

---

## References and links

1. D. L. Rockwell, "New directions for infrared countermeasures", *Aerospace Am.* **44**, 22 (2006).
2. K. S. Arnold and C. Y. She, "Metal fluorescence lidar (light detection and ranging) and the middle atmosphere", *Contemp. Phys.* **44**, 35 (2003).
3. Z. M. Liao, S. A. Payne, J. Dawson, A. Droboschoff, C. Ebberts, D. Pennington, and L. Taylor, "Thermally induced dephasing in periodically poled KTP frequency-doubling crystals", *J. Opt. Soc. Am. B* **21**, 2191 (2004).
4. O. A. Louchev, N. E. Yu, S. Kurimura, and K. Kitamura, "Thermal inhibition of high-power second-harmonic generation in periodically poled LiNbO<sub>3</sub> and LiTaO<sub>3</sub> crystals", *Appl. Phys. Lett.* **87**, 131101 (2005).
5. N. E. Yu, C. Jung, D.-K. Ko, J. Lee, O. A. Louchev, S. Kurimura, and K. Kitamura, "Thermal dephasing of quasi-phase-matched second-harmonic generation in periodically poled stoichiometric LiTaO<sub>3</sub> at high input power", *J. Korean Phys. Soc.* **49**, 528 (2006).
6. H. Furuya, A. Morikawa, K. Mizuuchi, and K. Yamamoto, "High-beam-quality continuous wave 3 W green-light generation in bulk periodically poled MgO:LiNbO<sub>3</sub>", *Jpn. J. Appl. Phys.* **45**, 6704 (2006).
7. S. V. Tovstonog, S. Kurimura, and K. Kitamura, "Continuous-wave 2 W green light generation in periodically poled Mg-doped stoichiometric lithium tantalate", *Jpn. J. Appl. Phys.* **45**, L907 (2006).
8. M. M. Fejer, G. A. Magel, D. H. Jundt, and R. L. Byer, "Quasi-phase-matched second harmonic generation: Tuning and tolerances", *IEEE J. Quantum Elect.* **28**, 2631 (1992).
9. G. D. Boyd and D. A. Kleinman, "Parametric interaction of focused Gaussian light beams", *J. Appl. Phys.* **39**, 3597 (1968).
10. M. V. Pack, D. J. Armstrong, and A. V. Smith, "Measurement of the  $\chi^{(2)}$  tensors of KTiOPO<sub>4</sub>, KTiOAsO<sub>4</sub>, RbTiOPO<sub>4</sub>, and RbTiOAsO<sub>4</sub> crystals", *Appl. Opt.* **43**, 3319 (2004).
11. I. Shoji, T. Kondo, A. Kitamoto, M. Shirane, and R. Ito, "Absolute scale of second-order nonlinear-optical coefficients", *J. Opt. Soc. Am. B* **14**, 2268 (1997).
12. D. Eimerl, "Thermal aspects of high-average-power electrooptic switches", *IEEE J. Quantum Elect.* **23**, 2238 (1987).
13. Y. Furukawa, K. Kitamura, S. Takekawa, A. Miyamoto, M. Terao, and N. Suda, "Photorefractive in LiNbO<sub>3</sub> as a function of [Li]/[Nb] and MgO concentrations", *Appl. Phys. Lett.* **77**, 2494 (2000).

## 1. Introduction

Wavelength conversion using periodically-poled (PP) nonlinear crystals has opened the way for a number of new technologies. A potentially useful and compact system is a fiber laser whose light is converted to a desired wavelength by PP nonlinear crystals. Such systems could be used on airplanes for infrared countermeasures against heat-seeking missiles [1] or in atmospheric studies as transportable sodium lidar systems for measurements of the middle atmosphere [2]. For these applications, high output powers are desirable. However, studies characterizing the behavior of PP nonlinear crystals at high powers have produced seemingly contradictory results. For example, several studies have shown that thermal dephasing in PP nonlinear crystals can severely degrade second-harmonic (SH) conversion efficiency when input fundamental power approaches 10 W [3-5]. On the other hand, recent experimental measurements of PP MgO-doped lithium niobate (PPMgLN) [6] and PP MgO-doped stoichiometric lithium tantalate (PPMgSLT) [7] saw no evidence of thermal dephasing for input fundamental powers of 8 W (for PPMgLN) and 11 W (for PPMgSLT). Since our principle interest is high-power applications of frequency-converted lasers, reliable characterization of the behavior of PP nonlinear crystals at high powers is vital.

In this work, we investigate the behavior of three commercial PP nonlinear crystals over a range of continuous-wave (CW) input powers up to 10 W. For comparison, the same fiber laser is used as the fundamental source for all three crystals. While we are interested in applications involving both parametric and harmonic frequency-conversion, this study focuses exclusively on frequency-doubling of 1064 nm light. The data is divided into two separate fundamental power regimes. Second-harmonic generation (SHG) data for fundamental powers less than 3 W is used to determine the effect of the fundamental laser linewidth and imperfections in periodic poling on SHG in the crystals. SHG data for fundamental powers between 3 and 10 W is used to study the consequences of thermal dephasing and pump depletion on frequency-doubling. These two effects are modeled theoretically, and results based on the model are compared to experimental data.

## 2. Experiment

The experimental setup is shown in Fig. 1. A linearly-polarized 10 W, 1064 nm Yb-doped fiber laser made by IPG Photonics is the fundamental light source. This small-footprint fiber laser can be used for the types of applications in which we are interested. The linewidth of the laser, which we measured to be 0.064 nm FWHM, is constant over the laser's power-tuning range. For the low fundamental power data sets ( $P_0 \leq 3$  W), the fiber laser was set to a constant output power of 3 W, and laser power through the crystals was adjusted with a waveplate and a polarizer. For high fundamental power ( $3 \text{ W} \leq P_0 \leq 10$  W), laser power through the crystals was adjusted by changing the output power of the fiber laser. The crystals used in the experiment were  $1 \times 2 \times 30 \text{ mm}^3$  PP potassium titanyl phosphate (PPKTP) made by Raicol, and  $1 \times 2.3 \times 30 \text{ mm}^3$  PPMgSLT and  $0.5 \times 3 \times 50 \text{ mm}^3$  PPMgLN, both made by HC Photonics. The crystals were placed on a copper stage that was temperature-controlled by a thermoelectric cooler to an accuracy of  $\pm 0.05$  °C. To insure temperature uniformity across the crystals, a copper cover was placed on top of the crystals, and direct thermal contact was made between the crystals and the copper cover with thermal grease. A 25 cm focal length

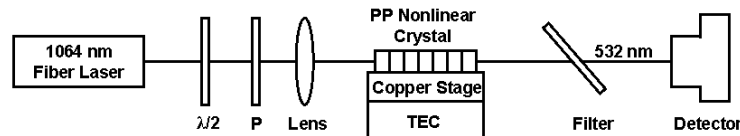


Fig. 1. Experimental setup. The  $\lambda/2$  plate and polarizer P were only used in the low fundamental power ( $P_0 \leq 3$  W) data runs.

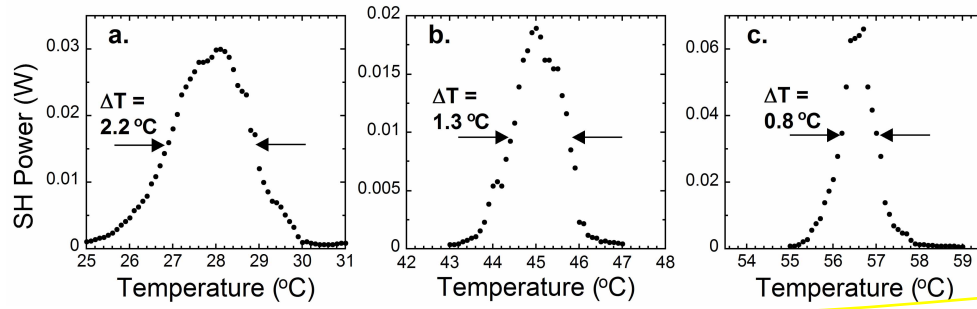


Fig. 2. Temperature tuning curves for (a) PPKTP, (b) PPMgSLT, and (c) PPMgLN, taken with approximately 1 W fundamental power through the crystals.

lens focused the fundamental light into the crystals, and a dichroic mirror separated fundamental and SH light exiting the crystals. SH power was measured with either a power meter or a silicon photodiode. The same experimental set-up was used for all three crystals to keep experimental conditions consistent, reducing variability when comparing data from different crystals.

### 3. SHG at low fundamental powers

Temperature tuning curves are shown in Fig. 2 when approximately 1 W of fundamental light is directed through the crystals. For fundamental powers less than 3 W, the average widths (FWHM) of the temperature tuning curves are  $2.18 \pm 0.03$  °C for PPKTP,  $1.34 \pm 0.04$  °C for PPMgSLT, and  $0.79 \pm 0.05$  °C for PPMgLN. Temperature tuning curve widths can be calculated for single-frequency light with the following equation [8]:

$$\Delta T = \frac{0.4429\lambda_{\omega}}{L} \left[ \frac{\partial n_{2\omega}}{\partial T} - \frac{\partial n_{\omega}}{\partial T} - \beta(n_{2\omega} - n_{\omega}) \right]^{-1} \quad (1)$$

*Handwritten notes: "at 30m" with an arrow pointing to L, and "W" with an arrow pointing to the right side of the equation.*

where  $\Delta T$  is the width of the temperature tuning curve,  $\lambda_{\omega}$  is the wavelength in vacuum of the fundamental light,  $L$  is crystal length,  $n_{\omega}$  and  $n_{2\omega}$  are the fundamental and SH indices of refraction, and  $\beta$  is the crystal's thermal expansion coefficient. The equation is evaluated at the optimum phase-matching temperature. Eq. (1) predicts temperature tuning curve widths of  $\Delta T = 1.55$  °C for PPKTP, 1.08 °C for PPMgSLT, and 0.63 °C for PPMgLN. The ratios of the calculated to the measured  $\Delta T$  are 0.71 for PPKTP, 0.81 for PPMgSLT, and 0.80 for PPMgLN.

Fig. 3 shows SH conversion efficiency as a function of fundamental laser power for each of the crystals. Also shown in Fig. 3 are linear fits to each of the data sets. The slopes of the lines are equal to the normalized SH conversion efficiencies,  $\eta$ , for each of the crystals. Based on the linear fits,  $\eta = 2.90 \pm 0.12$  %/W for PPKTP,  $2.08 \pm 0.09$  %/W for PPMgSLT, and  $5.64 \pm 0.12$  %/W for PPMgLN. Normalized SH conversion efficiency can be calculated theoretically for single-frequency light [9]:

$$\eta = \frac{P_{2\omega}}{(P_{\omega})^2} = \frac{16\pi^2 d_{\text{eff}}^2 L}{\lambda_{\omega}^3 n_{\omega} n_{2\omega} \epsilon_0 c} f \quad (2)$$

where  $P_{\omega}$  and  $P_{2\omega}$  are the fundamental and SH powers,  $d_{\text{eff}}$  is the effective nonlinear coefficient,  $\epsilon_0$  is the permittivity of vacuum,  $c$  is the speed of light, and  $f$  is the Boyd-Kleinman focusing factor. For the focusing conditions of this experiment,  $f$  is 1.00 for

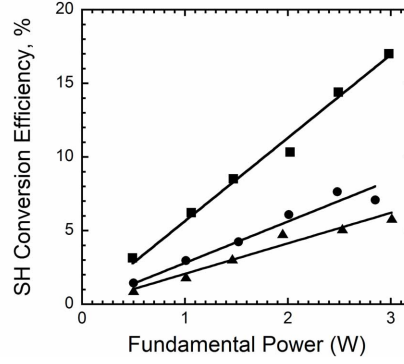


Fig. 3. SH conversion efficiency as a function of fundamental power for PPMgLN (squares), PPKTP (circles), and PPMgSLT (triangles). Also shown are linear fits to the data.

PPKTP, 0.90 for PPMgSLT, and 1.05 for PPMgLN. The duty cycle of each of the three crystals is 50%, making the effective nonlinearity of the crystals equal to [8]:

$$d_{\text{eff}} = \frac{2}{\pi} d_{33} \quad (3)$$

Previous studies have measured nonlinear coefficients of  $d_{33} = 15.4$  pm/V for KTP [10], 15.7 pm/V for MgSLT [5], and 25.0 pm/V for MgLN [11], resulting in effective nonlinearities of  $d_{\text{eff}} = 9.8$ , 10.0, and 15.9 pm/V for PPKTP, PPMgSLT, and PPMgLN respectively. Putting these values into Eq. (2) gives  $\eta = 4.11$  %/W for PPKTP, 2.82 %/W for PPMgSLT, and 13.7 %/W for PPMgLN, much greater than the measured  $\eta$ .

One possible reason for the disparity between the measured and calculated values of  $\eta$  is that the 0.064 nm linewidth of the fiber laser limits SHG in the crystals. The wavelength acceptance bandwidth of the crystals is found using the following equation [8]:

$$\Delta\lambda_{\text{crystal}} = \frac{0.4429\lambda_{\omega}}{L} \left| \frac{n_{2\omega} - n_{\omega}}{\lambda_{\omega}} + \frac{\partial n_{\omega}}{\partial \lambda} - \frac{1}{2} \frac{\partial n_{2\omega}}{\partial \lambda} \right|^{-1} \quad (4)$$

where the derivatives are evaluated at their respective wavelengths. This equation gives wavelength acceptance bandwidths of 0.089 and 0.083 nm for 30 mm PPKTP and PPMgSLT, respectively, and 0.042 nm for 50 mm PPMgLN. According to Ref. 8, when the properties of the PP nonlinear crystal or fundamental laser deviate from ideal, SH power falls as a  $\text{sinc}^2$  function in the limiting case where the fundamental light passing through the crystal is undepleted. This limiting case is justified when SH conversion efficiencies are low. Therefore, the SH power generated by a fundamental wavelength  $\lambda$  that is shifted from the ideal wavelength  $\lambda_0$  is equal to:

$$P_{2\omega} = P_{2\omega, \text{ideal}} \text{sinc}^2 \left[ 0.8858\pi \left( \frac{\lambda - \lambda_0}{\Delta\lambda_{\text{crystal}}} \right) \right] \quad (5)$$

where  $P_{2\omega, \text{ideal}}$  is the SH power generated by fundamental light at  $\lambda_0$ . Eq. (5) is only valid for single-frequency fundamental light. Any real-life laser will output light over a range of wavelengths. For the fiber laser used in this experiment, the distribution of wavelengths was measured to have a Gaussian profile:

$$P(\lambda) = \frac{0.94}{\Delta\lambda_{\text{laser}}} \exp \left[ -2.772 \left( \frac{\lambda - \lambda_0}{\Delta\lambda_{\text{laser}}} \right)^2 \right] \quad (6)$$

where  $\Delta\lambda_{\text{laser}}$  is the FWHM linewidth of the fiber laser. The equation has been normalized for a total output power of 1. For simple SHG, one can calculate SH power by solving the convolution integral of Eq. (5) and Eq. (6). However, sum-frequency generation could also have significant contribution to the output power at wavelengths around the SH wavelength. In order to account for sum-frequency generation, one must calculate a double convolution integral:

$$P_{\text{SFG}} = \int_0^\infty \int_0^\infty P(\lambda') P(\lambda'') P_{2\omega, \lambda' + \lambda''} d\lambda' d\lambda'' \quad (7)$$

where  $P_{2\omega, \lambda' + \lambda''}$  is found by making a substitution in Eq. (5):

$$P_{2\omega, \lambda' + \lambda''} = P_{2\omega, \text{ideal}} \text{sinc}^2 \left[ 0.8858\pi \left( \frac{\frac{\lambda' + \lambda''}{2} - \lambda_0}{\Delta\lambda_{\text{crystal}}} \right) \right] \quad (8)$$

Fig. 4 plots  $P_{\text{SFG}}$  as given by Eq. (7) over a range of  $\Delta\lambda_{\text{laser}}$ , where the linewidth of the laser has been normalized to the acceptance bandwidth of the crystal and  $P_{\text{SFG}}$  has been normalized to the ideal SH power for an infinitely narrow laser centered at  $\lambda_0$ . For PPKTP, the linewidth of the fiber laser is 0.72 of the acceptance bandwidth of the crystal, which, according to Eq. (7), will result in SH power which is 0.89 that of the ideal case of an infinitely narrow laser centered at  $\lambda_0$ . Similar calculations for PPMgSLT and PPMgLN give SH powers which are 0.88 and 0.68, respectively, that of the ideal case. Comparing measured values of normalized SH conversion efficiencies with the values calculated using Eq. (2) gives ratios of 0.71 for PPKTP, 0.74 for PPMgSLT, and 0.41 for PPMgLN. Therefore, while the non-zero linewidth of the fiber laser can account for part of the deviation from ideal SHG in the crystals, other effects must also be considered to explain the total deviation.

In addition to reducing SH power, the non-zero linewidth of the fiber laser can also broaden the crystals' temperature tuning curves. One can make a simple estimate of the width of the temperature tuning curve by treating temperature offset as a wavelength shift in Eq. (8):

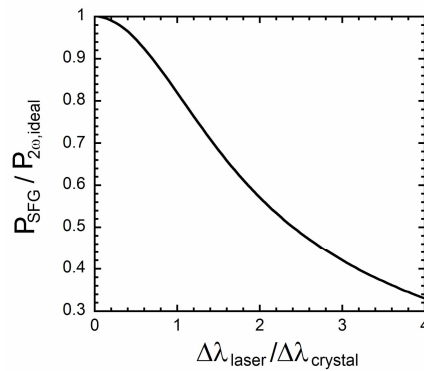


Fig. 4. SH output power from a PP nonlinear crystal as a function of laser linewidth. The calculation assumes that sum-frequency generation as well as SHG may occur. Output power is normalized to the calculated SH power generated by a laser with infinitely narrow linewidth, and laser linewidth is normalized to the wavelength acceptance bandwidth of the crystal.

$$P_{2\omega, \lambda'+\lambda''} = P_{2\omega, \text{ideal}} \text{sinc}^2 \left\{ 0.8858\pi \left[ \frac{\frac{\lambda'+\lambda''}{2} - \lambda_0 + \left( \frac{T-T_0}{\Delta T} \right) \Delta\lambda_{\text{crystal}}}{\Delta\lambda_{\text{crystal}}} \right] \right\} \quad (9)$$

where  $T$  is crystal temperature,  $T_0$  is the crystal temperature that maximizes SH power, and  $\Delta T$  is the width of the crystal's temperature tuning curve as determined by Eq. (1). Putting Eq. (9) into the convolution integral given in Eq. (7) gives temperature tuning curve widths of 1.70 °C for PPKTP, 1.20 °C for PPMgSLT, and 0.90 °C for PPMgSLT. As expected, the inclusion of the linewidth of the laser in the calculation results in broadening of the temperature tuning curves, which is in better agreement with our experimental measurements. Comparing the values of  $\Delta T$  given by Eqs. (7) and (9) to our measured values (see Fig. 1), one finds that the temperature tuning curve widths predicted by the convolution integral are 0.78, 0.90 and 1.1 of the measured temperature tuning curve widths for PPKTP, PPMgSLT, and PPMgLN, respectively. For PPKTP and PPMgSLT, the larger widths of the measured temperature tuning curves compared to those predicted by the convolution integral are probably due to the effective interaction lengths,  $L_{\text{eff}}$ , of the crystals being shorter than the actual lengths of the crystals. Following the method of Ref. 8, we calculate that a systematic chirp of 0.09%, or 2.5 pm between adjacent domains, will cause a 20% reduction in  $L_{\text{eff}}$  of PPKTP, which could account for the difference between the measured and predicted temperature tuning curve widths. Such a reduction in  $L_{\text{eff}}$  coupled with the above-discussed losses due to the linewidth of the fiber laser can also explain the difference between measured normalized SH conversion efficiencies for PPKTP and PPMgSLT and those predicted by Eq. (2).

For PPMgLN, the temperature tuning curve width predicted by the convolution integral is slightly broader than what is measured in the experiment. While it is impossible for  $L_{\text{eff}}$  to be larger than the length of the crystal, at the very least this result indicates that  $L_{\text{eff}}$  does not appear to be less than the crystal length. However, our experimental data indicate that SH conversion efficiency is significantly less than what is predicted by theory, even when the fiber laser linewidth is taken into account. A possible cause could be that the effective nonlinearity of the crystal is less than the ideal  $d_{\text{eff}}$  calculated with Eq. (3). This reduction in  $d_{\text{eff}}$  could be caused by spreading or smearing of the domains during poling.

#### 4. SHG at high fundamental powers

Fig. 5 shows temperature tuning curves for PPKTP, PPMgSLT, and PPMgLN when fundamental powers between ~3 W and ~10 W are sent through the crystals. The shifting of the PPKTP and PPMgLN curves as fundamental power increases indicates thermal dephasing [3,5]. Thermal dephasing occurs when light is absorbed by the crystal, resulting in a non-uniform temperature distribution that degrades quasi-phase matching. Fig. 6 shows SH conversion efficiency as a function of fundamental light power for the three crystals. The solid line in Fig. 6 represents a linear increase in SH conversion efficiency with fundamental power, as happens at low fundamental powers (see Fig. 3). There is significant drop-off from this linear relationship as fundamental power increases beyond 5 W. In addition to thermal dephasing, another effect that reduces conversion efficiency is depletion of the fundamental (pump) power across the crystal. The dotted line in Fig. 6 shows the behavior of SH conversion efficiency when pump depletion is taken into account. While data for PPMgSLT does not show the shift in temperature tuning curves at high fundamental powers which is characteristic of thermal dephasing [5], the measured SH conversion efficiency at high fundamental powers is still much less than that predicted by the pump depletion model. Therefore, some thermal dephasing probably occurs in PPMgSLT as well, although it does not result in shifting of the temperature tuning curves. The effect on SHG from thermal dephasing was calculated using a simple model which assumes that warming of the crystal due to

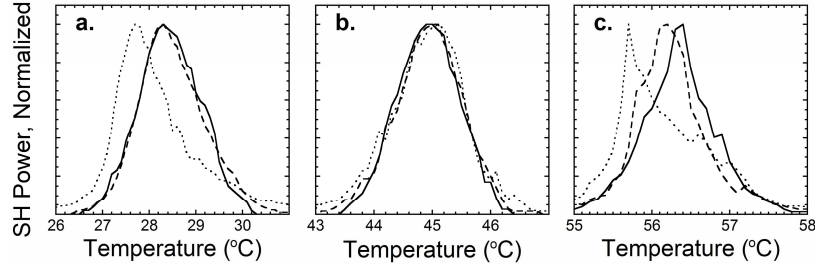


Fig. 5. Temperature tuning curves for (a) PPKTP, (b) PPMgSLT, and (c) PPMgLN. For PPKTP and PPMgSLT, the input fundamental powers are  $P_0 \sim 4.5$  W (solid line),  $P_0 \sim 6.5$  W (dashed line), and  $P_0 \sim 10.0$  W (dotted line). For PPMgLN, the input fundamental powers are the same except  $P_0 \sim 8.3$  W (dotted line).

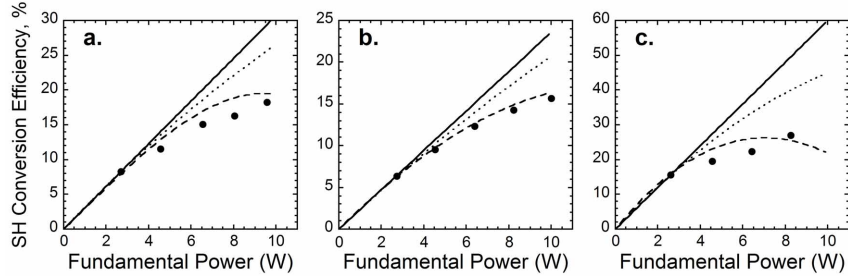


Fig. 6. SH conversion efficiency as a function of fundamental power for (a) PPKTP, (b) PPMgSLT, and (c) PPMgLN. Also shown are model fits that show a linear increase of SH conversion efficiency (solid line), SH conversion efficiency when pump depletion is taken into account (dotted line), and SH conversion efficiency when pump depletion and thermal dephasing are taken into account (dashed line).

absorption of light creates a temperature difference between the heating stage and the crystal. The magnitude of this temperature difference is calculated by solving the following Poisson's equation [12]:

$$\nabla^2 T = -\frac{P_{\text{heat}}}{VK} \quad (10)$$

where  $P_{\text{heat}}$  is heat power generated by light absorption,  $V$  is the volume of the crystal, and  $K$  is the thermal conductivity of the crystal. Following the method used in Ref. 3, the crystal is assumed to be a long cylinder and the laser beam passing through the crystal is assumed to be flat-top, with constant intensity out to the beam waist and zero intensity elsewhere. With these assumptions, solving Eq. (10) for temperature is analogous to finding electric potential outside a uniformly charged solid cylinder:

$$T_{\text{crystal}} - T_{\text{stage}} = \frac{P_{\text{heat}}}{4\pi L K} \left[ 1 + 2 \ln \left( \frac{a/2}{w_0/\sqrt{2}} \right) \right] \quad (11)$$

where  $L$  is the crystal length,  $a$  is the crystal width, and  $w_0$  is the beam waist, which is divided by  $\sqrt{2}$  because it is the SH beam, rather than the fundamental beam, which is predominantly absorbed.  $P_{\text{heat}}$  was found to a first-order approximation by solving the coupled fundamental and SH amplitude evolution equations with absorption included but without thermal dephasing. Power lost through absorption is assumed to go completely into heating of the crystal. The temperature difference between the crystal and the heating stage found using Eq. (11) was then used to calculate the effect of thermal dephasing on SHG in each of the crystals. The results of the calculation are shown as dashed lines in Fig. 6. The fact that other studies at similar fundamental laser powers did not see thermal dephasing effects [6,7] suggests that it may be possible to obviate thermal dephasing by carefully controlling crystal growth to reduce light-absorbing defects and, in the case of PPMgLN, using a stoichiometric crystal, which has better thermal properties than the congruent PPMgLN used in this study [13].

## 5. Conclusions

We have compared SHG in three different PP nonlinear crystals for fundamental powers up to 10 W in order to better understand the behavior of PP nonlinear crystals for high power applications. Based on data at low fundamental powers ( $P_0 \leq 3$  W), the normalized SH conversion efficiency was found to be appreciably less than that predicted by theory. Several possible causes were examined for this reduction in conversion efficiency. The linewidth of the 1064 nm fiber laser was found to reduce SH power by about 10% for PPKTP and PPMgSLT and by about 30% for PPMgLN. For PPKTP and PPMgSLT, the SH conversion efficiency may be further reduced by chirping of the periodicity of the poled domains, while for PPMgLN, smearing of the poled domains, which reduces the crystal's effective nonlinearity, could result in lower SH conversion efficiency. Data at high fundamental powers ( $3 \text{ W} \leq P_0 \leq 10 \text{ W}$ ) shows that SH conversion efficiency is further reduced by pump depletion and thermal dephasing in the crystals. Each of these effects are modeled and compared to experimental data, and good agreement is found. The data shows that even PPMgSLT, which did not have the shifting in its temperature tuning curves that is characteristic of thermal dephasing, still had significant degradation in SH conversion efficiency at high fundamental powers due to thermal dephasing. While previous studies suggest that thermal dephasing may be avoided by using carefully-prepared homemade crystals, the time and cost involved in such preparation makes such a solution problematic for commercial or military applications.